APPLIED GEOPHYSICS, Vol.13, No.1 (March 2016), P. 156-165, 9 Figures.
DOI:10.1007/s11770-016-0528-2

# Relationship between the transition frequency of local fluid flow and the peak frequency of attenuation*

Cao Cheng-Hao[1], Zhang Hong-Bing♦[1], Pan Yi-Xin[1], and Teng Xin-Bao[1]

**Abstract**: Local fluid flow (LFF) at the mesoscopic scale is the main dissipation mechanism of seismic waves in heterogeneous porous media within the seismic frequency band. LFF is easily influenced by the structure and boundary conditions of the porous media, which leads to different behaviors of the peak frequency of attenuation. The associated transition frequency can provide detailed information about the trend of LFF; therefore, research on the transition frequency of LFF and its relationship with the peak frequency of the corresponding attenuation (i.e., inverse of quality factor) facilitates the detailed understanding of the effect of inner structures and boundary conditions in porous media. In this study, we firstly obtain the transition frequency of fluid flux based on Biot's theory of poroelasticity and the fast Fourier transform algorithm in a sample containing one repeating unit cell (RUC). We then analyze changes of these two frequencies in porous media with different porous properties. Finally, we extend our analysis to the influence of the undrained boundary condition on the transition frequency and peak frequency in porous media with multiple RUCs. This setup can facilitate the understanding of the effect from the undrained boundary condition. Results demonstrate that these two frequencies have the same trend at low water saturation, but amplitude variations differ between the frequencies as the amount of saturation increases. However, for cases of high water saturation, both the trend and the amplitude variation of these two frequencies fit well with each other.
**Keywords**: Local fluid flow, peak frequency, transition frequency, saturation, boundary condition

## Introduction

When a fast P-wave travels across a heterogeneous porous medium containing inhomogeneities, the passing seismic wave induces a fluid pressure gradient between regions with different compliances. The resulting pressure gradients induce fluid flow; thus, part of the energy involved in the wave propagation is lost (Deng et al., 2012; Kudarova et al., 2013; Tisato and Quintal, 2013). This mechanism is referred as local fluid flow (LFF), and it is the major cause of attenuation and velocity dispersion at seismic frequencies in porous media at the mesoscopic scale (Guerriero et al., 2013; Quintal, 2012; Quintal et al., 2011; Rubino et al., 2014). As a result, accurate modeling of LFF at interfaces can facilitate the resolution of seismic data (Wang, 2011).

LFF in porous media has been studied extensively,

Manuscript received by the Editor June 20, 2015; revised manuscript received December 16, 2015.
*The research work is supported by National Natural Science Foundation of China (Grant No. 41374116) and the Fundamental Research Funds for Central Universities (Grant No. 2014B39014).
1. College of Earth Science and Engineering, Hohai University, Nanjing 211100, China.
♦Corresponding author: Zhang Hong-Bing (Email: hbzhang@hhu.edu.cn)
© 2016 The Editorial Department of **APPLIED GEOPHYSICS**. All rights reserved.

and such studies can generally be categorized as either analytical or numerical solutions in their characterization of LFF. For example, White and co-authors (White, 1975; White et al., 1975) first considered the attenuation and velocity dispersion caused by fluid flow in a poroelastic medium composed of two periodically alternating layers (patchy model). Ba et al. (2011) then derived a wave equation for dual-porosity media that clearly describes the attenuation and velocity dispersion in porous media; this can be considered to be compatible with the above-mentioned theory. Subsequently, Ba (2013) summarized and reviewed the effect of LFF in unsaturated-rock on seismic attributes, and the associated analytical solution is suitable for use in a simple pore medium model. The latter study is focused on the numerical solutions for characterizing the LFF, which is creep test (Masson et al., 2006; Quintal et al., 2011), oscillatory test (Rubino et al., 2009), and the use of poro-mechanism numerical modeling (Vogelaar and Smeulders, 2007). These methods can be used for more complex porous media, and both analytical and numerical solutions are mainly generated using an extension of Biot's equation of poroelasticity.

A viscoelastic model is commonly used to describe the behavior of anelastic effects. Examples of this are the Zener model (Zener and Siegel, 1949; Picotti et al., 2010; Quintal et al., 2011) and the standard linear solid model (Carcione and Picotti, 2006), where viscoelastic material properties are usually quantified in terms of their relaxation time, or spectrum of relaxation times. In this respect, it is essential to understand the transition frequency when predicting the way in which seismic velocities change in heavy oil reservoirs (Mavko, 2013). Usually, physical parameters (i.e., phase velocity and fluid flux) in relation to frequency dispersion have low- and high-frequency limits, and the transition frequency lies in the transitional zone between these two limits (Ba, 2013), thereby separating them. Thus, this frequency corresponds to the maximum absolute value of first derivate of the fluid flux versus frequency.

As the diffusion length becomes equal to the scale of the heterogeneities, attenuation caused by the LFF reaches a peak value. The frequency corresponding to this peak attenuation is known as the peak frequency (Müller et al., 2010; Rubino et al., 2013), and this explicitly provides information about the scale of heterogeneity and the properties of rocks. Most authors give expressions of peak frequency; for example, White and co-authors (White, 1975; White et al., 1975) proposed the patchy model and provided peak frequency based on this model, and Gelinsky et al. (1998) studied the effective bulk modulus based on the 1-dimensional poroelastic medium and obtained the corresponding peak frequency according to the effective bulk modulus.

LFF is easily influenced by other factors, and thus the frequency-dependency of attenuation may behave differently in accordance with these. Rubino et al. (2009) believed that differences in the distribution of fluid within a patchy reservoir leads to a different peak value and peak frequency of attenuation using the same average saturation. This is because a different distribution of the patchy reservoir change the behavior of the LFF, which may cause errors when obtaining the value of attenuation and peak frequency of attenuation, and will, in turn, have a negative influence on the estimation of saturation. In this respect, Quintal et al. (2012) selected only the core area (which occupies only 1/25 of the total area of the sample) to obtain the value of attenuation; they did so because the undrained boundary may affect the behavior of the LFF close to the boundary. To achieve this, it is necessary to discard the part of the model affected by the undrained boundary, and doing so involves an excessive use of computation resources. However, the resulting gain in the understanding of the distribution of the LFF will ultimately facilitate the understanding of the influence of the inner structure on the physical parameters (i.e., atteuation) and the influence range of the boundary thereby saving computation resources.

Aki and Richards (1980) proposed another definition for the quality factor that is based on the concept of energy loss and which can obtain the trend of the inverse quality factor versus frequency at a local scale, as well as the peak frequency at peak attenuation. Solazzi et al. (2014) used this approach to estimate the seismic attenuation distribution due to LFF, and it is considered that this method could inspire the construction of attenuation models for complex arrangements of heterogeneities. In addition, Deng et al. (2012) adopted solid velocity, pore pressure, and other parameters to describe changes in LFF, although such parameters can only describe the behavior of LFF at a series of frequencies and cannot reflect the trend of LFF under different porous parameters as well as boundary conditions. As a result, there are no parameters that can be used to accurately demonstrate LFF distribution and changes of fluid flux, and knowledge of these is critical for understanding the influence of the boundary condition on seismic attenuation and velocity dispersion.

In this study, we attempt to obtain the transition frequency of LFF, the values of which are derived from fluid flux using the finite difference method (Masson

et al., 2006) based on Biot's poroelastic equations. We seek to analyze the relation between transition frequency of the LFF and the associated peak frequency under situations of varying saturation in a single repeating unit cell (RUC). We also explore the influence of the undrained boundary condition and analyze the change trend and amplitude of the transition frequency of LFF in multiple RUCs with different saturations and porosity ratios. Finally, we explain and discuss the relationship between two types of frequencies in a layered porous media.

## Fluid flux within the low-frequency band

The seismic frequency band corresponds to a range of 1–100 Hz; as the low-frequency band at a mesoscopic scale ranges from 1 to 10 kHz, the low-frequency band is thus within the range of the seismic frequency band. Fluid flux can be referred to as the volume of a fluid at a unit time within a unit area that is induced by the pressure gradient, and it shows a good linear relationship with pore pressure in the low-frequency band (Mavko et al., 2009). Fluid flux can be expressed as follows:

$$Fluid\ \ flux(t) = abs\left(\frac{\kappa}{\eta}\nabla p\right), \tag{1}$$

where $p$ is pore pressure, $\nabla p$ is the fluid pressure gradient, $\kappa$ is permeability, and $\eta$ is viscosity (Müller and Rothert, 2006). However, it is not easy to realize equation (1) due to a series of computation errors that occur in relation to the truncated error of $\nabla p$.

Biot's quasi-static equations of consolidation, where inertial forces are excluded, can be obtained in the low-frequency band from Biot's equation of poroelasticity (Quintal et al., 2011). We can get the relative fluid velocity based on Biot's quasi-static equations in $t$ as follows:

$$V_{fz} = -\frac{\kappa}{\eta}\nabla p. \tag{2}$$

To simplify the computation here, we adopt relative fluid velocity to represent fluid flux at the low-frequency band, and therefore avoid using the computation implicit in equation (1). The unit of fluid flux in the paper omits time (s), and the corresponding unit is represented as displacement (m/s) (Liu et al., 2009). As fluid flux is presented using a time span, to explore the transition frequency of the *fluid flux* we therefore need to obtain the absolute value of the *fluid flux* (3) in the frequency domain using fast Fourier transform, as

$$Fluid\ \ flux = abs(FFT(V_{fz})). \tag{3}$$

## Numerical simulation and analytical result using single RUC

### Setup of model parameters and single RUC

In this section, all saturation cases shown in Figure 1 are introduced as follows. The medium consists of two different layers with different sets of solid frame properties, S1 and S2; S1 is saturated with water, while S2 is a gas. Six samples are arranged with increasing water saturation, which ranges from 31% (case 1) to 86% (case 6) in the layer of solid frame, S2. Variations in water saturation in this layered porous media are obtained by varying the thickness of S1. In addition, we chose to use an undrained boundary condition, as this is consistent with the symmetry of such media. This therefore implies that no fluid flow occurs at extremities of the RUCs with multiple courses of LFFs (Milani et al., 2014).

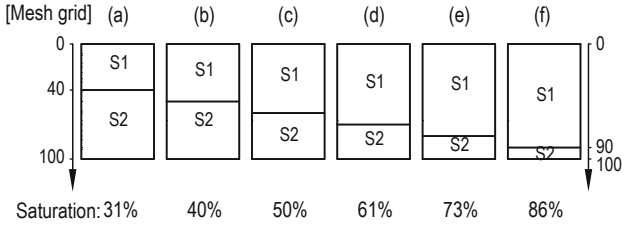


**Fig.1 Sketch of six rock samples with different levels of saturation; the scale 0–100 represents the spatial element, where Δz is 8e-3 m.**

In a single RUC model, the following parameters are chosen for numerical simulation: temporal interval $\Delta t$ = 5e − 7 s, spatial step $\Delta z$ = 8e − 3 m. The total time is 1s, which means the minimum frequency resolution is 1 Hz in the frequency domain. With the algorithms proposed by Masson et al. (2006), we carry out numerical simulations at each grid point by solving equations of motion using a staggered-grid finite-difference method at the fourth- and second-order in space and time, respectively.

The shear modulus of the dry frame, μ, is estimated as in Quintal, 2012:

$$\mu_2 = \frac{\mu_1}{K_{d1}} K_{d2}, \tag{4}$$

where subscripts 1 and 2 are used for properties of the solid frames S1 and S2, respectively; $K_d$ is the bulk modulus of the frame.

Assuming that grain diameter and tortuosity of the pore space is equal for both solid frames S1 and S2, equation (5) is then used for the approximation of permeability:

$$k_2 = k_1 \frac{\left(1-\phi_1\right)^2}{\phi_1^3} \frac{\phi_2^3}{\left(1-\phi_2\right)^2}. \tag{5}$$

**Table 1 Parameters of porous medium model**

| Parameters of grain and frame | Sandstone I (S1) | Sandstone II (S2) |
|---|---|---|
| Grain | | |
| Grain bulk modulus (GPa) | $K_s = 36.0$ | $K_s = 36.0$ |
| Grain density (kg·m$^{-3}$) | $\rho_s = 2650$ | $\rho_s = 2650$ |
| Frame | | |
| Dry rock bulk modulus (GPa) | $K_d = 9.5$ | $K_d = 7.6$ |
| Dry rock shear modulus (GPa) | $M = 9$ | Equation (4) |
| Porosity | $\Phi = 0.2$ | $\Phi = 0.3$ |
| Permeability(m$^2$) | $k = 5.0\text{e}-12$ | Equation (5) |

**Table 2 Physical properties of fillings**

| Physical parameters | Water | Gas |
|---|---|---|
| Grain density (kg·m$^{-3}$) | $\rho_w = 1040$ | $\rho_g = 78$ |
| Bulk modulus (GPa) | $K_w = 2.25$ | $K_g = 0.012$ |
| Viscosity (Pa·s) | $\eta_w = 0.003$ | $\eta_g = 0.00015$ |

It is of note that the wetting fluid, which in this context is water, preferentially saturates regions with small pores due to the capillary effect (Goertz and Knight, 1998).

## Distribution characteristics of fluid flux

To facilitate our understanding of the distribution of LFF, we analyze a single RUC with only one LFF course. We propose the concept of the LFF transition frequency based on use of the creep test. Transition frequency can describe the behavior of fluid flux, and it has two frequency limits, i.e. the fluid flux has constant values at both high and low frequency limits (Figure 2a). Therefore, the transition frequency can act as one frequency that distinguishes the two limits (Figure 2a), and based on the creep test it corresponds to the maximum absolute value of the first derivate of the fluid flux versus frequency (Figure 2a). It is of note that the transition frequency proposed in Figure 2a is quite different from that described in Müller and Rothert (2006).

Figure 2a demonstrates the distribution characteristics of fluid flux. In general, we can observe two transition frequencies: $f_{ff1}$ and $f_{ff2}$ in Figure 2a; the former, $f_{ff1}$, corresponds to the fluid flux related to the water in the S1 layer, while the latter, $f_{ff2}$, is caused by gas in the S2 layer. This verifies the conclusion made by Brajanovski et al. (2006) that attenuation can be interpreted as the superposition of two coupled diffusion processes in a fractured porous medium (one from the background and one from fractures embedded in background rock). Both $f_{ff1}$ and $f_{ff2}$ may contribute to the peak frequency of 1/Q; however, the amplitude corresponding to $f_{ff2}$ is smaller than that of $f_{ff1}$ occurring in layer S1. Therefore, in our models we adopt $f_{ff1}$ as the effective transition frequency of LFF.

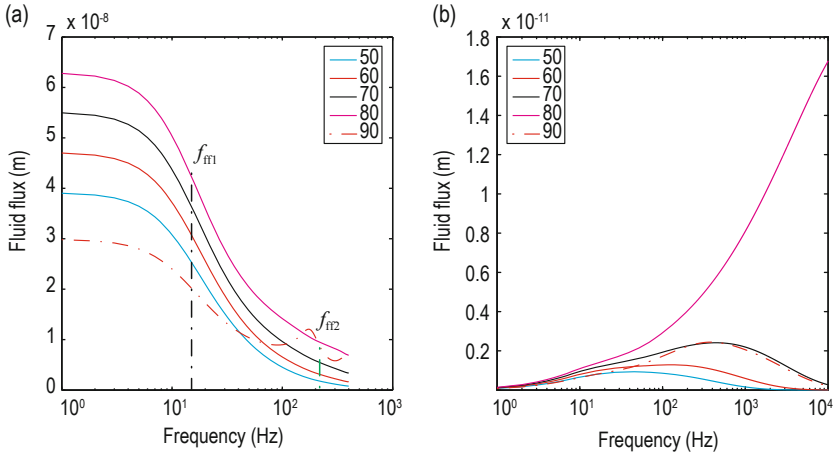


**Fig.2 Behavior of fluid flux (absolute value of $V_{fz}$) in frequency domain: (a) curves correspond to creep test result, and (b) White model. Numbers on legends correspond to those on left side of Figure 1.**

Figure 2b also describes the distribution of the LFF. However, the behavior of fluid flux (Figure 2b) is quite different to that determined using the creep test (Figure 2a), because the type of pressure on top of the sample (Müller and Rothert, 2006) is $\sigma(t) = p_e.exp(-iwt)$, which is different from that in the creep test of $\sigma(t) = p_e$, (where pe is the amplitude of the pressure, $i$ is the imaginary unit, and $t$ is time. It is thus evident that different forms of pressure lead to differing fluid flux behaviors (Figure 2).

In this study, we adopt the transition frequency based on the creep test to describe the behavior of LFF (maximum absolute value of the first derivate of the fluid flux in Figure 2a); the creep test is applicable for use with a complex poroelastic medium (Quintal et al., 2014), and the adoption of the creep test can facilitate determining the distribution of the LFF. In addition, an analysis of attenuation on the influence of peak frequency on a global scale can be brought about by determining changes in LFF, and an understanding of seismic attenuation sensitivity to the boundary condition can also be determined.

Please note, however, that the amplitude of pe has little influence on the transition frequency shown in Figure 2a.

## Characteristic frequency of LFF

For all cases listed in Figure 3, the transition frequency throughout the media is divided into two parts. The transition frequency in layer S2 has a greater fluctuation than that in layer S1, where the value of the frequency remains constant. Although this is a surprising observation, it can be explained as follows: layer S1 is saturated with water while S2 is saturated with gas, which is very compressible; therefore, the gas relaxation time is shorter than that of a fluid (Stephen, 2009). Compression causes flow from S1 into S2 (Kong et al., 2013). However, diffusion significantly decreases beyond the region of water diffusion, while fluid diffusion in S2 (dominated by gas) has a shorter relaxation time, i.e., the time taken to alter from the high frequency to low frequency limit is shorter for gas. Thus, the transition frequency ($f_{ff}$) for fluid flux can be seen to increase in layer S2 (in Figure 3).

Brajanovski et al. (2006) believed that superposition of two coupled LFFs in a porous medium leads to attenuation in a single RUC. In this respect, as the modulus of water is greater than that of gas (Table 2), it is considered that the general fluid flux would be dominated by LFF in the layer saturated with water.

In the work of Vogelaar and Smeulders (2007), the pore pressure gradient is determined to grow in line with extension of the length of the layer saturated with water. Therefore, it takes a longer time to reach equilibrium, and this corresponds to the smaller value of transition frequency required to equilibrate the fluid pressure between porous layers. As a result, we can observe that as water saturation increases, the transition frequency ($f_{ff}$) for the fluid flux decreases.

Porosity also plays a significantly role in oil and gas exploration. We therefore attempt to analyze the relationship between porosity and the transition frequency by varying the porosity of S1. In Figure 3, it can be observed that for smaller values of porosity in layer S1 (in case b) there is a smaller permeability according to equation (5); therefore the pressure gradient is lower than that in case a. Reduced porosity allows for a small amount of fluid flux from layer S1 to layer S2 (Brajanovski et al., 2005), and therefore in a layered porous media this process takes less time to equilibrate pore pressure. As a result, we observe a sharp increase in the transition frequency ($f_{ff}$) of fluid flux (Figure 3) at the point in the porous layer S2 (Figure 1).

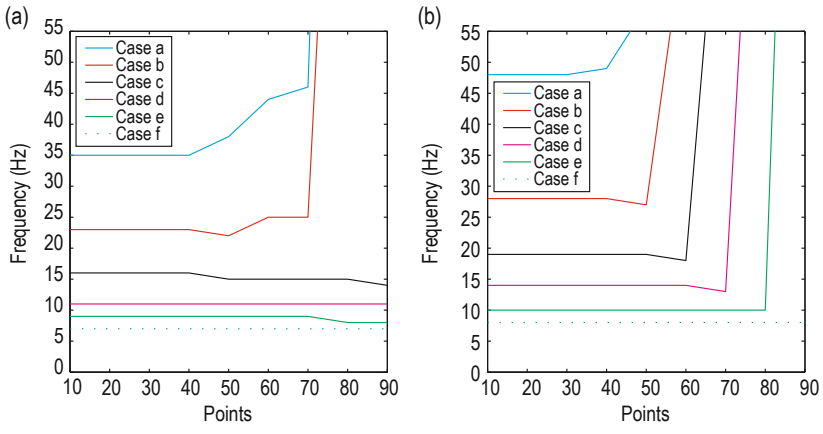


**Fig.3 Characteristic frequencies of fluid flux in six samples shown in Figure 1, with different porosity ratios: (a) porosity ratio $\varphi_2/\varphi_1$ = 1.5; (b) $\varphi_2/\varphi_1$ = 2.0.**

## Analysis of numerical results

The behavior of LFF is very different at various points within a complex media. The different behaviors of LFF can thus provide an insight into the inner structure of the medium. As a considerable amount of research has already been conducted on the peak frequency of attenuation, we select samples within a single RUC to study the relation between the transition frequency of LFF and the peak frequency of the associated attenuation. In doing so, we utilize the present achievement (6) relating to peak frequency to study the behavior of the LFF with the ultimate aim of facilitating our understanding of the inner structure of the medium.

Based on a comparison between Figures 4a and 4b, we observe that peak frequency, ($f_{tr}$), decreases in line with a decrease in the porosity ratio of $\varphi_2/\varphi_1$. Therefore, peak frequency behavior fits well with equation (6):

$$f_{tr} \approx \frac{8\kappa_1 K_{E1}}{\pi\eta_1 d_1^2}, \qquad (6)$$

where subscript 1 represents the water-saturated layer, d is the thickness of the layer, and KE is the effective modulus. Equation (6) describes behavior of the characteristic frequency, where the peak frequency is proportional to the effective modulus of the wave-saturated layer, and the effective modulus varies inversely with porosity $\varphi$ (Picotti et al., 2010). Thus, peak frequency is inversely related to porosity $\varphi$.

Since attenuation in a porous media in seismic frequency band is mainly caused by the mesoscopic LFF effect, research on the relation between LFF behavior on a mesoscopic scale and attenuation can facilitate construction of attenuation models for complex arrangements of heterogeneities.

Based on fluid flux behavior, it is possible to obtain the transition frequency, fwi, for the course of a LFF. To better quantify the relationship between the transition frequency, ($f_{wi}$), and the peak frequency, ($f_{tr}$), seven numerical simulations with water saturation ranging from 22% to 86% are performed under different porosity ratios to explore the relationship between these two frequencies. The porosity for the S1 layer is fixed for all these simulations. The results for $\varphi_2/\varphi_1 = 1.5$ are shown in Figure 4a, and those of $\varphi_2/\varphi_1 = 2$ are shown in Figure 4b.

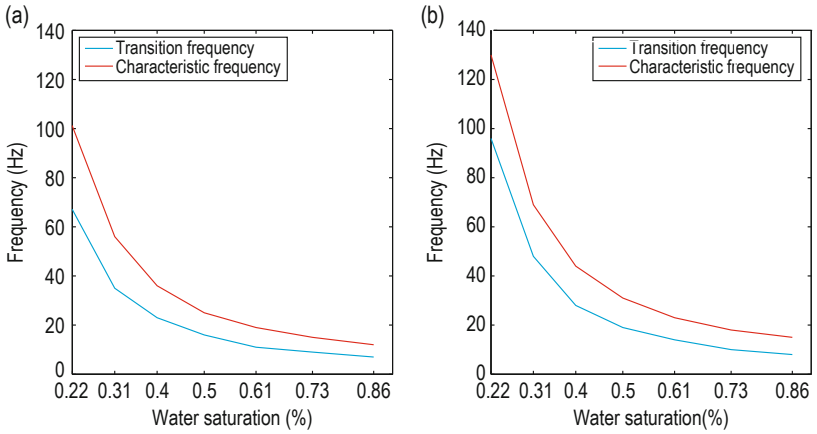


**Fig.4 Behavior of transition frequency ($f_{wi}$) for LFF and peak frequency ($f_{tr}$) for attenuation in cases of (a) $\varphi_2/\varphi_1 = 1.5$, and (b) $\varphi_2/\varphi_1 = 2$.**

A comparison of the blue and red curves in Figure 4 shows that with an increase in water saturation, the peak frequency, ($f_{tr}$), of 1/Q is proportional to the transition frequency, ($f_{wi}$), for the LFF. This tendency is the same for both cases with different porosity ratios. This understanding can assist with obtaining information about peak frequency at a local scale, thereby avoiding the cumbersome and possibly error-prone parameterization of approximation functions. Therefore, even in unfavorable cases, it is possible that information relating to peak frequency ($f_{tr}$) of 1/Q is embedded in the transition frequency, ($f_{wi}$), of the LFF.

# Numerical simulation and analytical results of RUCs

In the previous section, samples containing only one RUC were analyzed. We now analyze the influence of an undrained boundary and extend our research into transition frequency and peak frequency behaviors for

cases of periodical layered porous media.

## Parameters established for RUCs

The rock samples studied have multiple alternating layers with different sets of solid frame properties, S1 and S2 (Table 1); the properties of fillings are listed in Table 2. The undrained boundary is chosen as the boundary condition. The local fluid flow is induced by pore pressure at the interface of an RUC with different physical properties; therefore, one RUC corresponds to one LFF course. We consider three types of rock samples containing different amounts of RUCs with different saturations, which are shown in Figure 5 as follows; rock samples containing 1, 6, and 8 RUCs are represented by the black, red, and green lines, respectively, and saturations in all of the models range from 40 to 86%.

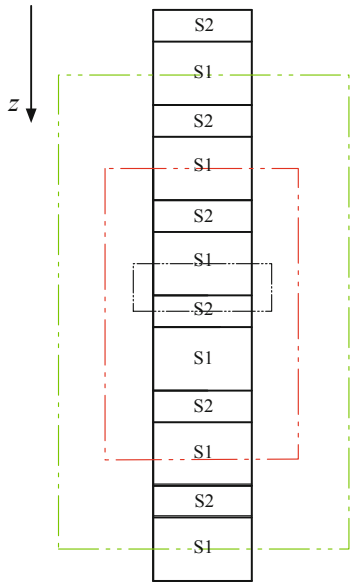


**Fig.5 Schematic representation of three RUCs: single RUC (black line), 6 RUCs (red line), 8 RUCs (green line).**

In this section, the variation in water saturation within such a layered porous media (Figure 6) is obtained by varying the relative thickness of the layers, S1, while fixing the general thickness of the RUCs.

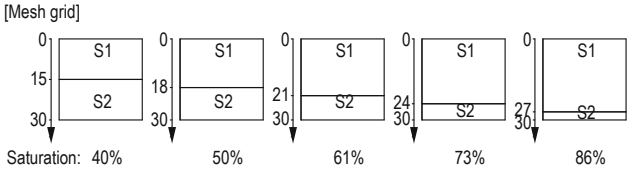


**Fig.6 Schematic illustration of different saturations for one RUC. Numbers on the left and right sides indicate spatial elements where the spatial element Δz is 8e − 3 m.**

## Results of transition frequency of LFF and peak frequency

Figure 7a shows the behaviors of the transition frequency, ($f_{wi}$), for samples with differing sizes of RUCs containing multiple RUCs and differing saturations. A comparison can thus be determined between the characteristic frequencies ($f_{wi}$) of multiple LFFs with the same saturation, and it is possible to determine that discrepancies between characteristic frequencies ($f_{wi}$) grow in line with a decrease in saturation. It is thus also possible to conclude that the single RUC (represented by asterisks in Figure 7) is unable to represent periodical layered media, particularly in cases with limited water saturation.

In contrast, the transition frequency, ($f_{wi}$), in the intermediate part of the samples is a little higher in the case containing 6 RUCs than in the case containing 8 RUCs. This disagreement can be explained by Müller and Rothert (2006), who propose the idea that the behavior of the original three-layer model with equant-thickness layers can be effectively modeled by a two-layer model with distinct layer thicknesses. Therefore, at the first stage of the diffusion process, the pressure gradient will equilibrate quickly between layers with similar properties, and at later times of the pore pressure diffusion process more and more of these equivalent layers merge and form a new set of larger equivalent layers with quite different equivalent porous layers. Thus, the original multiple-layer model with equant-thickness layers can be effectively modeled by a double-layer medium (Müller and Rothert, 2006).

For the two cases in Figures 7a and b, the transition frequency is highest at points close to the undrained boundary (1 and 6 on the X-axis in Figure 7a, and 1 and 8 on the X-axis in Figure 7b), than for other points, which are far away from the boundary; the transition frequency for the fluid flux is therefore smaller. This shows that the undrained boundary condition may give results of a significantly higher value than its counterpart points, particularly in conditions of low water saturation. Therefore, the transition frequency, ($f_{tr}$), for points in the intermediate part of the samples (Figure 5) avoid the influence of the undrained boundary condition, and are thus representative of the transition frequency for the corresponding periodical layered porous medium (Figure 7).

The behavior of the peak frequency of 1/Q is quite different for various sizes of RUCs containing multiple RUCs under the same water saturation, as shown in Figure 8. With an increase in water saturation,

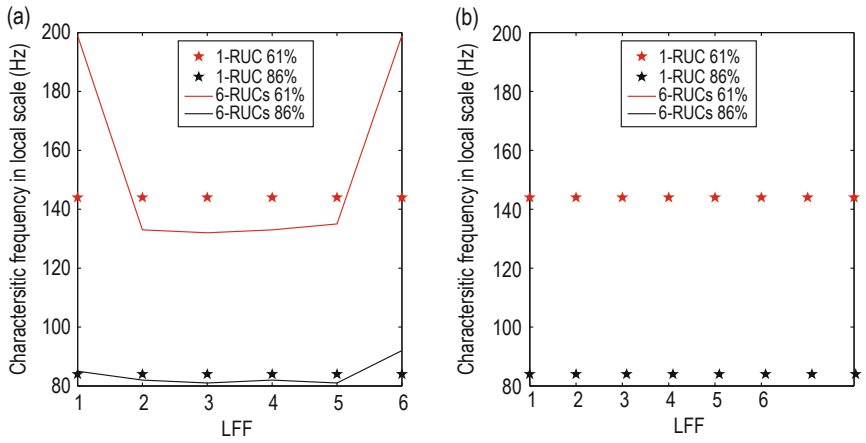


**Fig.7 Characteristic frequencies of LFFs for porous samples with respect to different RUCs (shown in X-axis). Points on X-axis range from 1 to 6 (a) and 1 to 8 (b) and correspond to different LFFs in 6 and 8 RUCs, respectively.**

discrepancies between different sizes of RUCs containing multiple RUCs decrease (Figure 8). As a result, peak frequency in the medium containing 8 RUCs can be treated as the most genuine value of the peak frequency for saturations ranging from 0.22 to 0.86. On the other hand, for the low water saturation, peak frequency discrepancies of 1/Q for different sizes of RUCs can no longer be neglected. This result does not fit well with the opinion proposed by Milani et al. (2014), who suggested that the peak frequency at which maximum attenuation occurs is not significantly affected by the size of RUCs.

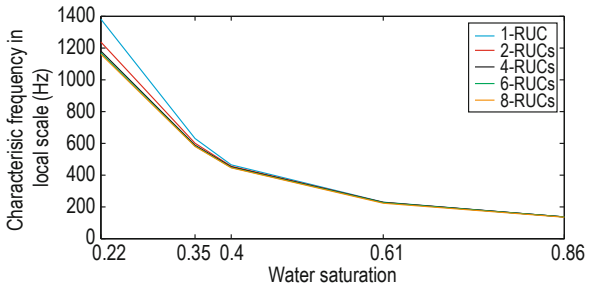


**Fig.8 Schematic illustration of peak frequency of attenuation with regard to saturation in layered porous media.**

However, results show that two kinds of frequencies (fwi and ftr) in the layered porous models share the similar trend as saturation decreases, but have different values of amplitudes (Figure 9). This phenomenon can be explained as follows. As the LFF is a superposition of two coupled fluid-diffusion processes, a smaller value of water saturation means an increase in the proportion of the fluid-diffusion process caused by the gas in S2. Therefore, our assumption that fff of the fluid flux in the water-saturated layer, S1, can be treated as the fwi of the LFF (see section "Distribution characteristics of the fluid flux") is no longer correct. Nonetheless, it is of note that this assumption (see section "Distribution characteristics of the fluid flux") is still correct in most ranges of saturation, and that the relationship between the ftr of 1/Q and $f_{wi}$, which is obtained through the water in S1, is correct.

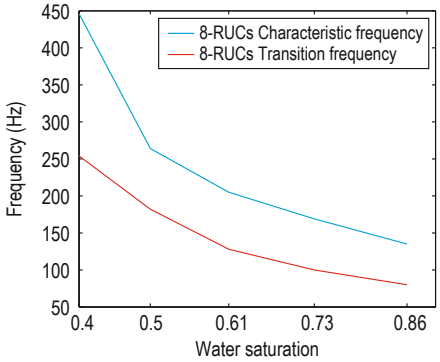


**Fig.9 Behaviors of transition frequency (fwi) and peak frequency (ftr) in cases of saturation ranging from 0.4 to 0.86 in media containing 8 RUCs.**

## Conclusions

In this paper, the methodology proposed by Masson et al. (2006) is adopted to explore the relation between the transition frequency of LFF and the peak frequency of the inverse quality factor in a single RUC and multiple RUCs, respectively. The following conclusions are

obtained:

(1) The fluid flux (equation (1)) is substituted by the relative velocity of the fluid flux (equation (2)). Although this is formally incorrect, it is a fact that the inertial part of the fluid flux, which can be almost neglected in a seismic frequency band, justifies this assumption, and hence allows for a valuable insight into the relationship between the transition frequency ($f_{wi}$) and the peak frequency ($f_{tr}$) of 1/Q.

(2) Although we already know the transition frequency ($f_{ff}$) of the fluid flux (Müller and Rothert, 2006), the trend of the transition frequency is not convenient for extracting a uniform parameter with which to characterize the fluid flux (Figure 2b). We thus propose a novel version of the fluid flux based on the creep test, which can facilitate description of the inner structure of the porous media (Figure 2a).

(3) If information is available in relation to variations in physical properties, it is possible that the undrained boundary condition can lead to a higher transition frequency of the LFF at points adjacent to the undrained boundary, and that the transition frequency of the LFF in the intermediate part of the models can represent the natural transition frequency in the periodical layered porous (Figure 7). Meanwhile, when there is an increase in the size of RUCs that contain multiple RUCs, the peak frequency (peak values of the attenuation) becomes close to one fixed value (Figure 8). Thus, the influence of the boundary condition on the transition frequency of the LFF, and the peak frequency of attenuation is similar; that is, as the size of RUCs containing multiple RUCs grows, the negative effect caused by the undrained boundary diminishes.

(4) The result presented is partly due to the assumption that we set the transition frequency of the water at the interface of the layers as the transition frequency for the LFF, but it demonstrates that the transition frequency of the LFF accords well with the peak frequency at a high water saturation level. However, it fails to show relations at a low water saturation level (Figure 9), where water accounts for a lower proportion in samples, although this result is beneficial to research relating to mesoscopic pore structure.

For the sake of simplicity, a periodical porous media was selected for the models. However, in actuality, real porous material is obviously more complex. Therefore, future research should be extended, and the relation proposed in this paper should be generalized to use a fluid-saturated porous medium with a random distribution of inhomogeneity.

# References


Aki, K., and Richards, G. P., 1980, Quantitative seismology: Theory and methods: W. H. Freeman, 162−163.

Ba, J., 2013, Progress and Review of Rock Physics, Tsinghua University Press, 150−212.

Ba, J., Carcione, J. M., and Nie, J. X., 2011, Biot-Rayleigh theory of wave propagation in double-porosity media: Journal of Geophysical Research Atmospheres, **116**(B6), 309–311.

Brajanovski, M., Gurevich, B., and Schoenberg, M., 2005, A model for P-wave attenuation and dispersion in a porous medium permeated by aligned fractures: Geophysical Journal International, **163**(1), 372−384.

Brajanovski, M., Müller, T. M., and Gurevich, B., 2006, Characteristic frequencies of seismic attenuation due to wave-induced fluid flow in fractured porous media: Geophysical Journal International, **166**(2), 574−578.

Carcione, J.M., and Picotti, S., 2006, P-wave seismic attenuation by slow-wave diffusion: Effects of inhomogeneous rock properties: Geophysics, **71**(3), O1−O8.

Deng, J. X., Wang, S. X., and Du, W., 2012, A study of the influence of mesoscopic pore fluid flow on the propagation properties of compressional wave-a case of periodic layered porous media: Chinese Journal of Geophysics (in Chinese), **55**(8), 2716−2727.

Gelinsky, S., Shapiro, S. A., Muller, T., and Gurevich, B., 1998, Dynamic poroelasticity of thinly layered structures. International Journal of Solids and Structures, **35**(34−35), 4739−4751.

Goertz, D., and Knight, R., 1998, Elastic wave velocities during evaporative drying: Geophysics, **63**(1), 171–183.

Guerriero, V., Mazzoli, S., Iannace, A., Vitale, S., Carravetta, A., and Strauss, C., 2013, A permeability model for naturally fractured carbonate reservoirs: Marine and Petroleum Geology, **40**, 115−134.

Kong, L., Gurevich, B., Muller, T.M., Wang, Y., and Yang, H., 2013, Effect of fracture fill on seismic attenuation and dispersion in fractured porous rocks: Geophysical Journal International, **195**(3), 1679−1688.

Kudarova, A. M., van Dalen, K. N., and Drijkoningen, G. G., 2013, Effective poroelastic model for one-dimensional wave propagation in periodically layered media: Geophysical Journal International, **195**(2), 1337−1350.

Liu, J., Ma, J. W., and Yang, H. Z., 2009, Research on dispersion and attenuation of P wave in periodic layered-model with patchy saturation: Chinese Journal of Geophysics (in Chinese), **52**(11), 2879–2885.

Müller, T.M., Gurevich, B., and Lebedev, M., 2010, Seismic

wave attenuation and dispersion resulting from wave-induced flow in porous rocks–A review: Geophysics, **75**(5), 75A147−75A164.

Müller, T.M., and Rothert, E., 2006, Seismic attenuation due to wave-induced flow: Why Q in random structures scales differently: Geophysical Research Letters, **33**(16), L16305.

Masson, Y.J., Pride, S.R., and Nihei, K.T., 2006, Finite difference modeling of Biot's poroelastic equations at seismic frequencies: Journal of Geophysical Research-Solid Earth, **111**(B10).

Mavko, G., 2013, Relaxation shift in rocks containing viscoelastic pore fluids: Geophysics, **78**(3), M19–M28.

Mavko, G., Mukerji, T., and Dvorkin, J., 2009, The Rock Physics Handbook, Second Edition, Cambridge University Press, 389–394.

Milani, M., Rubino, J. G., Quintal, B., Holliger, K., and Muller, T. M., 2014, Velocity and attenuation characteristics of P-waves in periodically fractured media as inferred from numerical creep and relaxation tests: 84th Ann. Internat. Mtg., Soc. Expl. Geophys., Expanded Abstracts, 2882−2887.

Picotti, S., Carcione, J.M., Rubino, J.G., Santos, J.E., and Cavallini, F., 2010, A viscoelastic representation of wave attenuation in porous media: Computers & Geosciences, **36**(1), 44−53.

Quintal, B., 2012, Frequency-dependent attenuation as a potential indicator of oil saturation: Journal of Applied Geophysics, **82**, 119–128.

Quintal, B., Jänicke, R., Rubino, J., Steeb, H., and Holliger, K., 2014, Sensitivity of S-wave attenuation to the connectivity of fractures in fluid-saturated rocks: Geophysics, **79**(5), WB15–WB24.

Quintal, B., Steeb, H., Frehner, M., and Schmalholz, S.M., 2011, Quasi-static finite element modeling of seismic attenuation and dispersion due to wave-induced fluid flow in poroelastic media: Journal of Geophysical Research, **116**(B1).

Quintal, B., Steeb, H., Frehner, M., Schmalholz, S. M. and Saenger, E. H., 2012, Pore fluid effects on S-wave attenuation caused by wave-induced fluid flow: Geophysics, **77**(3), L13–L23.

Rubino, J. G., Holliger, K., Guarracino, L., Milani, M., and Müller, T. M., 2014, Can we use seismic waves to detect hydraulic connectivity between fractures: 84th Ann. Internat. Mtg., Soc. Expl. Geophys., Expanded Abstracts, 2894–2898.

Rubino, J. G., Monachesi, L. B., Müller, T. M., Guarracino, L., and Holliger, K., 2013, Seismic wave attenuation and dispersion due to wave-induced fluid flow in rocks with strong permeability fluctuations: The Journal of the Acoustical Society of America, **134**(6), 4742–4751.

Rubino, J. G., Ravazzoli, C. L., and Santos, J.E., 2009, Equivalent viscoelastic solids for heterogeneous fluid-saturated porous rocks: Geophysics, **74**(1), N1–N13.

Solazzi, S., Guarracino, L., Germán Rubino, J., Milani, M., Holliger, K., and Müller, T., 2014, An energy-based approach to estimate seismic attenuation due to wave-induced fluid flow: 84th Ann. Internat. Mtg., Soc. Expl. Geophys., Expanded Abstracts, 1991–1995.

Stephen, R. A., 2009, Viscoelastic Waves in Layered Media: Journal of the Acoustical Society of America, **126**(6), 3374–3375.

Tisato, N., and Quintal, B., 2013, Measurements of seismic attenuation and transient fluid pressure in partially saturated Berea sandstone: evidence of fluid flow on the mesoscopic scale: Geophysical Journal International, **195**(1), 342–351.

Vogelaar, B., and Smeulders, D., 2007, Extension of White' s layered model to the full frequency range: Geophysical Prospecting, **55**(5), 685–695.

Wang, S. D., 2011, Attenuation compensation method based on inversion: Applied Geophysics, **8**(2), 150–157.

White, J., 1975, Computed seismic speeds and attenuation in rocks with partial gas saturation: Geophysics, **40**(2), 224–232.

White, J. E., Mihailova, N., and Lyakhovitsky, F., 1975, Low-frequency seismic waves in fluid-saturated layered rocks: Journal of the Acoustical Society of America, **57**(S1), S30–S30.

Zener, C. M., and Siegel, S., 1949, Elasticity and Anelasticity of Metals: The Journal of Physical and Colloid Chemistry, **53**(9), 1468–1468.

Cao Cheng-Hao received his BS from Nanjing University of Technology in 2009 and his MS from Hohai University in 2012. He is presently working as a Ph.D. Candidate in Hohai University, majoring in Geodetection and Information Technology. His research focuses on rock physics and its application.